A DISCONTINUOUS VELOCITY LEAST SQUARES FINITE ELEMENT METHOD FOR THE STOKES EQUATIONS WITH IMPROVED MASS CONSERVATION

JAMES LAI[§], PAVEL BOCHEV[¶], LUKE OLSON[‖], KARA PETERSON[**], DENIS RIDZAL[††], AND CHRIS SIEFERT[‡‡]

Abstract. Conventional least squares finite element methods (LSFEM) for incompressible flows conserve mass approximately. In some cases, this can lead to an unacceptable loss of mass and unphysical solutions. In this report we formulate a new, locally conservative LSFEM for the Stokes equations which computes a discrete velocity field that is point-wise divergence free on each element. To this end, we employ discontinuous velocity approximations which are defined by using a local stream-function on each element. The effectiveness of the new LSFEM approach on improved local and global mass conservation is compared with a conventional LSFEM employing standard C^0 Lagrangian elements.

1. Introduction. Least-squares finite element methods (LSFEMs) have been applied to incompressible flows with varying success. The key issue is that LSFEMs are residual minimization schemes and hence conserve mass only approximately. For some problem configurations, this can lead to an unacceptable loss of mass and unphysical solutions. A locally conservative mimetic LSFEM has been defined for the Stokes equations in [4] and [3, Section 7.7] using compatible finite element spaces. However, the mimetic LSFEM requires non-standard boundary conditions specifying the normal velocity and the tangential vorticity on the domain boundary. So far, it has not been extended to the more common and practically important velocity boundary condition and it is not clear whether or not this can be done.

Mass conservation in least squares methods for the Stokes equations with the velocity boundary condition has been studied extensively in literature [6, 9, 10, 13, 14, 15]. Loss of mass in LSFEMs can be countered by mesh refinement [13], high order elements [16], modifying the least-squares functional [15], weighting the continuity equation more strongly [10], or by enforcing it on each element by Lagrange multipliers [9]. However, neither one of these approaches can be deemed completely satisfactory.

Mass conservation does not improve proportionally with mesh refinement–leading to an impractical alternative. High order elements require an increased amount of storage and computation and the improvements to mass conservation are not commensurate with the additional cost [13, 15]. Modifying the least squares functional with terms that promote mass conservation has proven to be very successful [15], however, it is an ad hoc way of improving mass conservation and may depend on the problem on hand. Another alternative is to enforce element-wise mass conservation using Lagrange multipliers [9]. While this approach yields exact mass conservation on each element, it also results in a saddle-point system, thereby negating the main reason one may want to consider LSFEMs.

An idea that has not been explored much in the context of LSFEMs is the use of discontinuous elements. Discontinuous LSFEM can be viewed as generalizations of LSFEMs for transmission and mesh-tying problems; see [1], [3, Section 12.10] and [8], from a fixed number of subdomains to an arbitrary number of subdomains.

In this report we formulate, in two stages, a new locally conservative LSFEM for the Stokes equations with the velocity boundary condition by using discontinuous velocity approximations. Our starting point is a weighted L^2 least-squares formulation [2] employing

[§]University of Illinois at Urbana-Champaign, Department of Computer Science, jhlai2@illinois.edu
[¶]Sandia National Laboratories, pbboche@sandia.gov
[‖]University of Illinois at Urbana-Champaign, Department of Computer Science, lukeo@illinois.edu
[**]Sandia National Laboratories, kjpeter@sandia.gov
[††]Sandia National Laboratories, dridzal@sandia.gov
[‡‡]Sandia National Laboratories, csiefer@sandia.gov

conventional C^0 elements and the velocity-vorticity-pressure (VVP) form of the Stokes equations. The first stage relaxes the continuity of the velocity field only and adds new terms which penalize the normal and the tangential jumps of the velocity across the element interfaces. We show that by adjusting the relative importance of the normal and tangential jump terms this intermediate *discontinuous velocity* LSFEM can lead to noticeable improvements in the mass conservation. However, the weights required for improved mass conservation differ from problem to problem, thereby making this formulation insufficiently robust for practical problems.

At the second stage, we proceed to define the discontinuous velocity field on each element as the curl of a local stream-function. This guarantees that the velocity is pointwise divergence free on each element. Thus, our approach can be interpreted as implementation of the intermediate *discontinuous velocity* LSFEM using locally divergence free basis for the velocity. This idea bears some similarity with the *discrete* LSFEM in [7] with two crucial distinctions. First and foremost, the method in [7] is not a discontinuous formulation; in order to cope with the discontinuity in the approximating space this method replaces the differential operators by weak discrete versions defined using integration by parts. The second distinction is that we eliminate completely the velocity and work directly with the stream function, whereas [7] retains the original fields.

The resulting discontinuous stream-function-vorticity-pressure (SVP) LSFEM is locally conservative and offers a much improved global and local mass conservation compared to its parent LSFEM employing C^0 elements. We demonstrate the usefulness of the new formulation through a series of numerical examples.

1.1. Notation. For simplicity we restrict attention to two space dimensions and bounded, simply connected regions $\Omega \subset \mathbb{R}^2$ with Lipschitz-continuous boundary. In what follows we use the standard notation $H^k(\Omega)$ for the Sobolev space of all square integrable functions which have square integrable derivatives of orders up to k. The norm and inner product on H^k are $\|\cdot\|_k$ and $(\cdot,\cdot)_k$, respectively.

As usual, when $k = 0$ we write $L^2(\Omega)$, $(\cdot,\cdot)$ and $\|\cdot\|_0$. The symbol $H^1_0(\Omega)$ denotes a subspace of $H^1(\Omega)$ of functions whose trace vanishes on $\partial\Omega$ and $L^2_0(\Omega)$ is the subspace of L^2 fields with vanishing mean. The dual of $H^1_0(\Omega)$ is the space $H^{-1}(\Omega)$ with norm

$$\|u\|_{-1} = \sup_{v\in H^1_0(\Omega)} \frac{(u,v)}{\|v\|_1}\,. \tag{1.1}$$

Vector valued fields and their associated function spaces are denoted by bold face symbols, e.g., $\mathbf{u} = (u_1, u_2)$ is a vector field in two dimensions and $\mathbf{H}^1(\Omega)$ is the Sobolev space of vector fields with components are in $H^1(\Omega)$. In two dimensions, the curl is defined for scalar and vector functions as

$$\nabla\times\omega = \begin{bmatrix}\omega_y\\ -\omega_x\end{bmatrix}, \quad \nabla\times\mathbf{u} = \mathbf{u}_{2x} - \mathbf{u}_{1y}\,. \tag{1.2}$$

We use $\mathcal{K}$ to denote a partition of Ω into finite elements K. In two dimensions K can be a quadrilateral or a triangle and the interface between two elements is an edge e. The sets of all interior and boundary edges in the mesh are denoted by $\mathcal{E}(\Omega)$ and $\mathcal{E}(\Gamma)$, respectively. Finally, $\mathcal{E} = \mathcal{E}(\Omega)\cup\mathcal{E}(\Gamma)$ is the set of all edges in the mesh.

The standard C^0 finite element spaces of degree $r > 0$ on quadrilateral and triangular grids are denoted by Q_r and P_r, respectively. We will also need their discontinuous versions $[Q_r]$ and $[P_r]$. When the type of the element is not important we write R_r and $[R_r]$ with the understanding that $R_r = Q_r$ on quadrilaterals and $R_r = P_r$ on triangles.

Discontinuous finite element methods require various jump terms on element interfaces. Let K_+ and K_- be two adjacent elements that share edge e and denote the velocities on each element by $\mathbf{u}^+$ and $\mathbf{u}^-$ respectively. Define the jump in normal and tangential components across e as

$$[\mathbf{u}\cdot\mathbf{n}] = \mathbf{u}^+\cdot\mathbf{n}^+ + \mathbf{u}^-\cdot\mathbf{n}^-, \quad [\mathbf{u}\times\mathbf{n}] = \mathbf{u}^+\times\mathbf{n}^+ + \mathbf{u}^-\times\mathbf{n}^-. \tag{1.3}$$

where $\mathbf{n}^+$ and $\mathbf{n}^-$ are the outer normals on ∂K^+ and ∂K^- respectively. The jump of a scalar function is defined as usual by the difference

$$[\psi] = \psi^+ - \psi^-. \tag{1.4}$$

2. The continuous prototype least-squares method. In this section we review the weighted L^2 least-squares method for the Stokes equations which is the prototype for the discontinuous, locally conservative LSFEM. In terms of the primitive variables the governing equations assume the form

$$\begin{cases} -\triangle\mathbf{u} + \nabla p &= \mathbf{f} \quad \text{on } \Omega \\ \nabla\cdot\mathbf{u} &= 0 \quad \text{on } \Omega \end{cases} \tag{2.1}$$

where $\mathbf{u}$ and p are the velocity and the pressure, respectively, and $\mathbf{f}$ is a given vector function specifying the body force. The system (2.1) is augmented with the velocity boundary condition

$$\mathbf{u} = 0 \quad \text{on } \partial\Omega \tag{2.2}$$

and the zero mean pressure constraint

$$\int_\Omega p\, d\Omega = 0\,. \tag{2.3}$$

The first equation in (2.1) governs conservation of momentum while the second (continuity equation) governs conservation of mass.

Least-squares methods for (2.1), (2.2) and (2.3) are usually defined using an equivalent first-order form of the Stokes equations. This eliminates the need for globally H^2-conforming finite elements which require C^1 continuity and are difficult to construct. There are several first order formulations of the Stokes equations to choose from, the most common being the velocity-vorticity-pressure formulation in which the vorticity

$$\omega = \nabla\times\mathbf{u} \tag{2.4}$$

is introduced as a new variable. Using the identity,

$$\nabla\times\nabla\times\mathbf{u} = -\triangle\mathbf{u} + \nabla(\nabla\cdot\mathbf{u}) \tag{2.5}$$

and the continuity equation, we arrive at the velocity-vorticity-pressure (VVP) first order formulation of the Stokes equations

$$\begin{cases} \nabla\times\omega + \nabla p &= \mathbf{f} \quad \text{on } \Omega \\ \omega - \nabla\times\mathbf{u} &= 0 \quad \text{on } \Omega \\ \nabla\cdot\mathbf{u} &= 0 \quad \text{on } \Omega \end{cases} \tag{2.6}$$

The VVP system is augmented with the velocity boundary condition (2.2) and the zero mean constraint (2.3).

2.1. Weighed L^2 least-squares method. LSFEMs define unconstrained minimization problems via residual minimization over an appropriate Hilbert space. Thus, the LSFEM solution is given by the solution to the minimization of a norm-equivalent functional devised using the squares of the residuals of each equation of the partial differential equation in the appropriate norm. The resulting discretized system that minimizes the functional over the finite element subspace is guaranteed to be symmetric and positive definite.

One can show that for the VVP system with velocity boundary conditions, the negative norm functional

$$J_{-1}(\mathbf{u}, \omega, p; \mathbf{f}) = \|\nabla \times \omega + \nabla p - \mathbf{f}\|_{-1}^2 + \|\nabla \times \mathbf{u} - \omega\|_0^2 + \|\nabla \cdot \mathbf{u}\|_0^2 \tag{2.7}$$

is norm equivalent on $X_{-1} = [H_0^1(\Omega)]^2 \times L^2(\Omega) \times L_0^2(\Omega)$. A least squares principle for (2.6) is to minimize (2.7) over X_{-1}.

The negative norm (1.1) admits the following characterization [3].

Theorem 2.1. *For any $u \in H^{-1}(\Omega)$*

$$\|u\|_{-1}^2 = \left\|(-\triangle)^{-1/2} u\right\|_0^2 \tag{2.8}$$

This theorem reveals that the negative norm is not easily computable because it requires inversion of the Laplace operator. Therefore, to obtain a practical LSFEM it must be approximated. The diagonal operator

$$(-\triangle)^{-1/2} \mapsto h\mathcal{I} \tag{2.9}$$

gives a simple, yet sufficiently accurate for our purposes approximation of the negative norm [3]. Using (2.9) the first term of (2.7) is approximated by

$$\|\nabla \times \omega + \nabla p - \mathbf{f}\|_{-1}^2 \approx h^2 \|\nabla \times \omega + \nabla p - \mathbf{f}\|_0^2 \tag{2.10}$$

We arrive at the following discrete version of (2.7)

$$\begin{aligned} &J_{-1}^h(\mathbf{u}^h, \omega^h, p^h; \mathbf{f}) = \\ &\qquad h^2 \left\|\nabla \times \omega^h + \nabla p^h - \mathbf{f}\right\|_0^2 + \left\|\nabla \times \mathbf{u}^h - \omega^h\right\|_0^2 + \left\|\nabla \cdot \mathbf{u}^h\right\|_0^2 \end{aligned} \tag{2.11}$$

where $(u^h, \omega^h, p^h) \in X_r^h = [R_r(\Omega) \cap H_0^1(\Omega)]^2 \times R_{r-1}(\Omega) \cap H^1(\Omega) \times R_{r-1} \cap L_0^2(\Omega)$, $r > 1$. We refer to (2.11) as the weighted L_2 method[1] since it is composed of L_2 norms of the squares of the residuals of each equation scaled by an approximate mesh weight. In what follows we restrict attention to the lowest-order admissible space, i.e., $r = 2$.

One can show that (2.11) is well-posed and optimally convergent formulation [3]. In particular, the following theorem holds [3].

Theorem 2.2. *Let $(\mathbf{u}^h, \omega^h, p^h) \in X_2^h$ be a solution to (2.11), and $(\mathbf{u}, p, h) \in X$ be the exact solution to (2.6), such that $\mathbf{u} \in \mathbf{H}^3(\Omega)$, $\omega \in H^2(\Omega)$ and $p \in H^2(\Omega)$. There exists a constant $C > 0$ such that*

$$\left\|\mathbf{u} - \mathbf{u}^h\right\|_1^2 + \left\|\omega - \omega^h\right\|_0 + \left\|p - p^h\right\|_0 \leq Ch^2 \left(\|\mathbf{u}\|_3 + \|\omega\|_2 + \|p\|_2\right). \tag{2.12}$$

[1] For simplicity, in our implementation of the weighted method the one dimensional nullspace of the pressure is eliminated by setting the pressure on the boundary to zero at one point instead of enforcing (2.3). These two approaches to handling the one dimensional nullspace of the pressure are equivalent; however, the choice affects the convergence of the iterative method used to solve the system. A comparison can be found in [3].

From Theorem 2.2, we see that using a quadratic/biquadratic approximation for the velocity and linear/bilinear approximations for the vorticity and pressure result in optimal convergence rates. Nonetheless, for simplicity we work the equal-order version of the finite element space

$$\overline{X}_2^h = (R_2(\Omega) \cap H_0^1(\Omega))^2 \times R_2(\Omega) \cap H^1(\Omega) \times R_2 \cap L_0^2(\Omega)\,. \tag{2.13}$$

We use (2.11) as a basis for our discontinuous velocity LSFEM.

2.2. Mass conservation in the weighted L^2 least-squares method. Theorem 2.2 asserts that the weighted L^2 method is optimally accurate for all sufficiently smooth exact solutions of the Stokes equations. This means that asymptotically $\|\nabla \cdot u\| \to 0$, as $h \to 0$. However, on a given fixed mesh size this term cannot be guaranteed to be as small as may be required, nor could its convergence to zero be assured for insufficiently smooth velocity fields. In this section we show that these concerns are not unfounded and that in some cases mass loss in the weighted least-squares method can be significant.

To this end we consider two standard test problems: the backward-facing step flow, shown in Fig. 2.1, and a channel flow past a cylinder, shown in Fig. 2.2. For the backward-facing step problem the domain is the rectangle $[0, 10] \times [0, 1]$ with a reentrant corner at $(2, 0.5)$. The velocity boundary condition is specified as follows. On the inflow ($x = 0$) and outflow ($x = 10$) walls

$$\mathbf{u}_{in} = \begin{bmatrix} 8(y - 0.5)(1 - y) \\ 0 \end{bmatrix} \quad \text{and} \quad \mathbf{u}_{out} = \begin{bmatrix} y(1 - y) \\ 0 \end{bmatrix}, \tag{2.14}$$

respectively. Along all other portions of the boundary $\mathbf{u}_{wall} = \mathbf{0}$ is enforced.

The geometry of the second test problem is given by the rectangle $[-1, 3]\times[-1, -1]$ with a disk of radius $r = 0.6$ centered at $(0, 0)$, removed from the domain. The velocity boundary condition for this problem is set as follows. On the inflow ($x = -1$), outflow ($x = 3$), top ($y = 1$) and bottom ($y = -1$) sides

$$\mathbf{u}_{in} = \mathbf{u}_{out} = \mathbf{u}_{wall} = \begin{bmatrix} (1 - y)(1 + y) \\ 0 \end{bmatrix}. \tag{2.15}$$

and on the surface of the "cylinder" $\mathbf{u}_{cyl} = \mathbf{0}$. Therefore, velocity is set to zero on all parts of the boundary except for the inflow and the outflow portions of $\partial\Omega$.

Note that in both test problems specification of the velocity boundary condition is compatible with $\nabla \cdot \mathbf{u} = 0$ because fluid enters and leaves the domain only through the inflow and the outflow boundaries, respectively and

$$\int_{\Gamma_{in}} \mathbf{u}_{in} \cdot \mathbf{n}\, d\ell = \int_{\Gamma_{out}} \mathbf{u}_{out} \cdot \mathbf{n}\, d\ell \tag{2.16}$$

To assess the mass conservation properties of the least-squares methods considered in this report we measure the total mass flow across several vertical surfaces connecting the top and the bottom sides of the computational domains. The lines marked by "S" in Figures 2.1-2.2 show two typical examples of such surfaces for the two test problems. Because the greatest mass loss for the backward-facing step is expected near the reentrant corner we always place one of the surfaces at $x = 2$. For the second test problem we always measure the flow across the surface at $x = 0$ where the domain narrows due to the cylindrical cutout.

Because for both test problems velocity is zero on all parts of the boundary except Γ_{in} and Γ_{out}, from the divergence theorem it follows that

$$\int_{\Gamma_{in}} \mathbf{u} \cdot \mathbf{n}_{in}\, d\ell = \int_S \mathbf{u} \cdot \mathbf{n}_S\, d\ell\,. \tag{2.17}$$

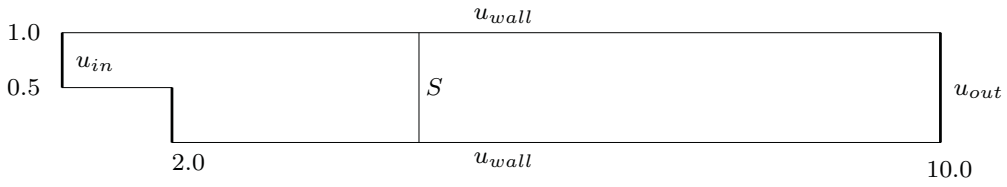

FIG. 2.1. *Geometry of the first test problem: backward-facing step.*

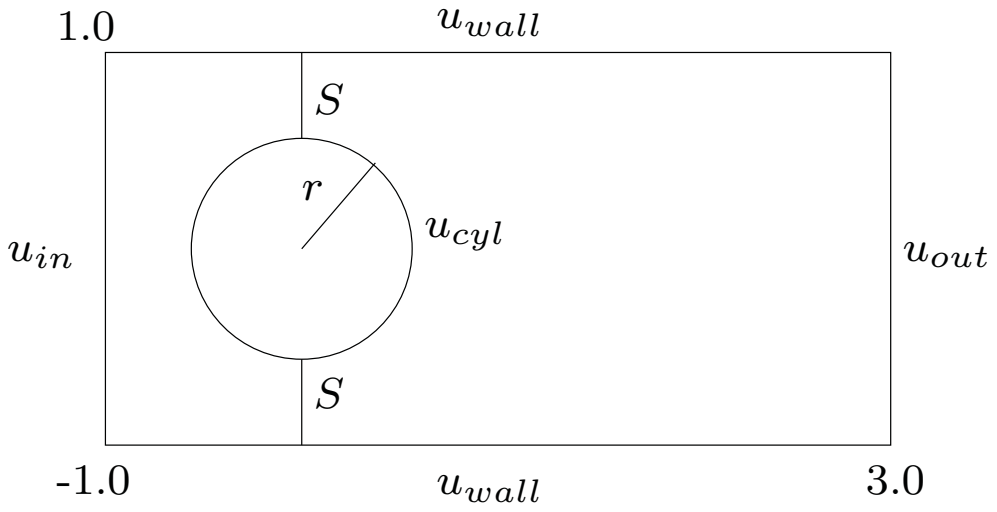

FIG. 2.2. *Geometry of the second test problem: flow past a cylinder.*

Therefore, mass conservation can be quantified by the precent mass loss across the surface S, defined as follows:

$$m_{loss} = \frac{\int_{\Gamma_{in}} \mathbf{u} \cdot \mathbf{n}_{in}\, d\ell - \int_{S} \mathbf{u} \cdot \mathbf{n}_{S}\, d\ell}{\int_{\Gamma_{in}} \mathbf{u} \cdot \mathbf{n}_{in}\, d\ell}. \tag{2.18}$$

To assess mass conservation properties of the weighted L^2 formulation we solve the two test problems using the following modified version of the weighted L^2 least-squares functional

$$\begin{aligned} J^h_\mu(\mathbf{u}^\mathbf{h}, \omega^h, p^h; \mathbf{f}^h) = \\ h^2 \left\| \nabla \times \omega^h + \nabla p^h - \mathbf{f}^h \right\|_0^2 + \left\| \nabla \times \mathbf{u}^h - \omega^h \right\|_0^2 + \mu \left\| \nabla \cdot \mathbf{u}^h \right\|_0^2 \end{aligned} \tag{2.19}$$

implemented using the equal order space (2.13). This modification has been proposed in [10] as a way to improve mass conservation in least-squares methods. By increasing μ we increase the relative importance of the residual of the continuity equation, thereby promoting mass conservation. In our study we use $\mu = 1$, $\mu = 10$ and $\mu = 20$.

Our results are summarized in Figure 2.3. We see that for $\mu = 1$ the least-squares solution of the backward-facing step problem experiences severe mass loss in excess of 50% of the total mass near the reentrant corner. Increasing μ does improve conservation, however, mass

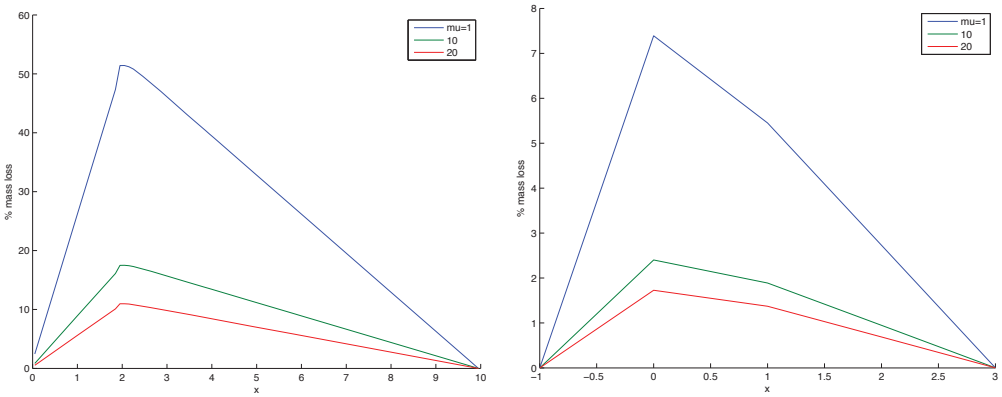

FIG. 2.3. *Percent mass loss of (2.19) for the backward-facing step (left panel) and the flow past a cylinder (right panel) test problems.*

loss remains unacceptably high even for $\mu = 20$. We note that significant increase of μ is not recommended as this will reduce the accuracy of the other terms in the functional and compromise, e.g., conservation of momentum. Indeed, by increasing the weight of a single term in the least squares functional, it is in effect *decreasing* the weight of the other terms. Thus, by choosing a large weight for μ to promote mass conservation, we are effectively demoting conservation of momentum. The mass loss in the second test problem is not as severe but still significant at 7%. In this case, setting $\mu = 20$ helps to bring down the loss of mass across the narrowings to about 2%.

REMARK 1. *Exact element-wise mass conservation with C^0 elements has been achieved in the so-called* restricted *least-squares method [9]. In the restricted LSFEM mass conservation on each element is added as an explicit constraint leading to the following constrained minimization problem:*

$$\begin{aligned} \min_{X_r^h} \quad & J_{-1}^h(\mathbf{u}^h, \omega^h, p^h; \mathbf{f}) \\ \text{subject to} \quad & \int_K \left(\nabla \cdot \mathbf{u}^h\right) dK = 0, \quad \forall K \in \mathcal{K} \end{aligned} \tag{2.20}$$

Although (2.20) returns a solution with exact element-wise mass conservation, the system is typically solved using Lagrange multipliers and results in a saddle-point system which negates the advantages of using least-squares in the first place. The constrained optimization problem can also be solved by a penalty approach, in which case one is led back to a formulation similar to (2.19) with a very large μ. Because the penalty must be strong enough to enforce the constraint accurately, the penalty formulation of (2.20) suffers from the same disadvantages as (2.19).

In the next section we explore an alternative approach to improve mass conservation in least-squares methods based on allowing discontinuous velocity spaces in the formulation.

3. Discontinuous velocity least-squares finite element method. Numerical results in the last section show that least-squares methods with C^0 elements can suffer from severe mass loss which in some cases may exceed 50% of the total mass. Furthermore, the remedies available to counter this loss are not satisfactory: weighting strongly the continuity equation residual as in (2.19) reduces conservation of momentum, while using the restricted formulation (2.20) leads to a saddle-point problem and negates the advantages of least-squares.

The option of using div-conforming elements to achieve exact mass conservation in least-squares methods has been explored in [4]. However, the resulting mimetic LSFEM requires

non-standard boundary conditions for the Stokes equations, and its extension to the practically important velocity boundary condition is not clear.

Consequently, in order to improve mass conservation in LSFEMs for the Stokes equation with the velocity boundary condition we propose to employ a *discontinuous* finite element approximation of the velocity, while retaining C^0 elements for the rest of the variables. In so doing we achieve two objectives. First, we keep the growth of the degrees of freedom to a minimum, compared to a fully discontinuous formulation. Second, relaxation of the interelement continuity of the velocity space allows a greater flexibility in the choice of the local finite element approximation of that variable. In particular, it becomes possible to consider locally divergence-free spaces which would have been impractical if the global velocity space had to be H^1-conforming.

Following these ideas we develop a *discontinuous* velocity least-squares finite element method based on the well-posed formulation (2.11) in two stages. At the first stage we allow discontinuous finite elements for the velocity in (2.11), i.e., we set

$$\widetilde{X}_r^h = ([R]_r)^2 \times R_{r-1} \times R_{r-1} \,. \tag{3.1}$$

This necessitates some changes in the least-squares functional, namely, the last two terms have to be broken into element sums to deal with the loss of conformity in the velocity space:

$$\begin{aligned} &\widetilde{J}_{-1}^h(\mathbf{u}^{\mathbf{h}}, \omega^h, p^h; \mathbf{f}^h) = \\ &\qquad h^2 \left\| \nabla \times \omega^h + \nabla p^h - \mathbf{f}^h \right\|_0^2 + \sum_{K \in \mathcal{K}} \left(\left\| \nabla \times \mathbf{u}^h - \omega^h \right\|_{0,K}^2 + \left\| \nabla \cdot \mathbf{u}^h \right\|_{0,K}^2 \right) \end{aligned} \tag{3.2}$$

Furthermore, to obtain a well-posed formulation with a unique solution, we need to recover some of the H^1-conformity qualities of the velocity. Therefore, constraints on the jumps in normal and tangential components of the velocity are introduced.

Recall that $\mathcal{E}(\Omega)$ is the set of all interior edges in the mesh. It is easy to see that the weighted L^2 least-squares method (2.11) is equivalent to the following constrained minimization problem

$$\begin{aligned} &\min_{\widetilde{X}_r^h} \widetilde{J}_{-1}^h(\mathbf{u}^h, \omega^h, p^h; \mathbf{f}^h) \\ &\text{subject to } \int_{e_i} [\mathbf{u}^h \cdot \mathbf{n}_i] d\ell = 0 \quad \text{and} \quad \int_{e_i} [\mathbf{u}^h \times \mathbf{n}_i] d\ell = 0 \quad \forall e_i \in \mathcal{E}(\Omega) \end{aligned} \tag{3.3}$$

The constrained system can be solved by Lagrange multipliers in which case the resulting minimization problem becomes

$$\min_{\widetilde{X}_r^h} \max_{\mathbb{R}^{|\mathcal{E}|}} \widetilde{J}_{-1}^h(\mathbf{u}^h, \omega^h, p^h; \mathbf{f}^h) - \sum_{e_i \in \mathcal{E}(\Omega)} \lambda_1^i \int_{e_i} [\mathbf{u}_i \cdot \mathbf{n}_i] d\ell - \sum_{e_i \in \mathcal{E}} \lambda_2^i \int_{e_i} [\mathbf{u}_i \times \mathbf{n}_i] d\ell \tag{3.4}$$

Of course, similar to (2.20), this formulation is a saddle-point system that gives rise to an indefinite algebraic system.

Instead of using Lagrange multipliers we will encourage H^1 conformity by a penalty approach–by adding residuals of the interelement jumps to the least-squares functional. This gives rise to the following *discontinuous* velocity functional:

$$\begin{aligned} &\widehat{J}_{-1}^h(\mathbf{u}^h, \omega^h, p^h; \mathbf{f}^h) = \\ &\qquad h^2 \left\| \nabla \times \omega^h + \nabla p^h - \mathbf{f}^h \right\|_0^2 + \sum_{K \in \mathcal{K}} \left(\left\| \nabla \times \mathbf{u}^h - \omega^h \right\|_{0,K}^2 + \left\| \nabla \cdot \mathbf{u}^h \right\|_{0,K}^2 \right) \\ &\qquad + h^{-1} \sum_{e_i \in \mathcal{E}(\Omega)} \left(\alpha_1 \int_{e_i} [\mathbf{u} \cdot \mathbf{n}_i]^2 d\ell + \alpha_2 \int_{e_i} [\mathbf{u} \times \mathbf{n}_i]^2 d\ell \right) \end{aligned} \tag{3.5}$$

where $\alpha_1, \alpha_2 > 0$ are penalty parameters. The values of these constants can be used to adjust the relative importance of normal vs. tangential continuity.

Based on analogies with div-conforming elements, one could argue that strengthening the normal continuity of the velocity field should lead to improved mass conservation in the finite element solution of (3.5). If this were the case, then the discontinuous velocity formulation (3.5) with $\alpha_1 \gg \alpha_2$ should be able to take care of the mass losses in our two test problems. To test this hypothesis we implement (3.5) using the equal-order discontinuous velocity, continuous vorticity and pressure finite element space

$$[\overline{X}_2^h] = ([R_2])^2 \times R_2 \times R_2 \tag{3.6}$$

and solve the two test problems with two different choices for α_1 and α_2. The first choice is to set $\alpha_1 = \alpha_2 = 100$, in which case we expect[2] to see mass losses comparable to that in the C^0 formulation. The second set of weights is $\alpha_1 = 100$, $\alpha_2 = 0.01$ emphasizes normal over tangential continuity. If our hypotheses were correct, this set of weights would lead to a much improved mass conservation.

Unfortunately, the results shown in Fig. 3.1 refute our seemingly logical hypothesis. The

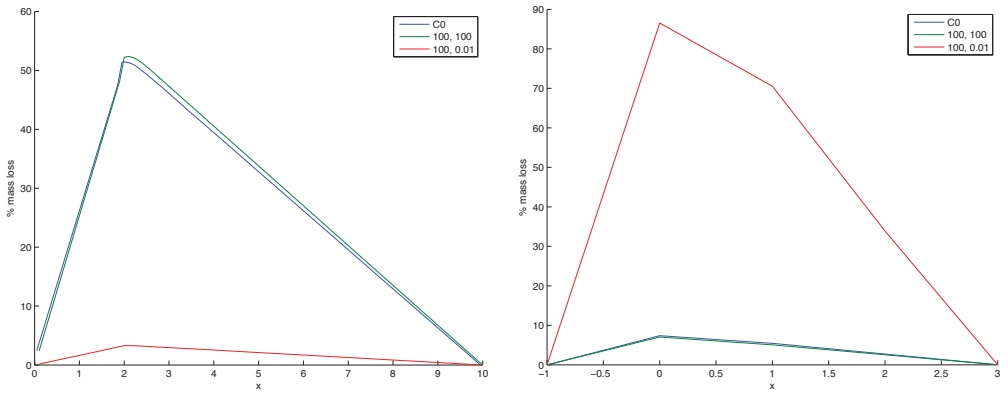

FIG. 3.1. *Percent mass loss in the discontinuous velocity least-squares method (3.5) for the backward-facing step (left panel) and the flow past a cylinder (right panel) test problems. Green line corresponds to* $\alpha_1 = \alpha_2 = 100$*, red line corresponds to* $\alpha_1 = 100$*,* $\alpha_2 = 0.01$ *and the blue line gives the reference mass loss by the* C^0 *least-squares method (2.11). The legend values are read as* α_1, α_2 *with (2.11) as reference labeled* (C_0)*.*

left panel in the figure shows that for the backward-facing step problem the second weight combination does lead to a *significant improvement* in the mass conservation by reducing the mass loss from over 50% to just a bit over 3%. However, for the flow past a cylinder the situation is completely reversed. Now the choice $\alpha_1 = 100$, $\alpha_2 = 0.01$ leads to a *significant deterioration* of the mass conservation and increases mass loss from 7% in the C^0 formulation to *nearly* 90%! These results clearly indicate that the discontinuous velocity formulation (3.5) cannot be reliably counted on to always reduce the mass loss with the same choice of weights, i.e., its mass conservation properties are problem dependent. This is an undesirable feature that we shall deal with at the second stage of the formulation of our new method.

To motivate this stage we note that while discontinuous velocity does allow for improvements in mass conservation, the least-squares formulation (3.5) does not enforce exact mass conservation on each element. At the same time, considering that the velocity space is not

[2]This is because in the limit as $\alpha_1 \to \infty$ and $\alpha_2 \to \infty$, (3.5) recovers the C^0 solution of the weighted L^2 LSFEM method.

subject to any interelement continuity, it is obvious that we have a greater flexibility in choosing the velocity representation on each element than in the C^0 setting. In particular, we can take advantage of this flexibility by choosing the velocity to be *pointwise* divergence free on each element by setting

$$\mathbf{u}^h|_K = \nabla \times \psi^h|_K \quad \forall K \in \mathcal{K}\,, \tag{3.7}$$

where $\psi^h \in [R]_r$ is a discontinuous *stream function*. Therefore, at the second stage we replace the velocity field in (3.5) with the field defined in (3.7). Note that when defining $\mathbf{u}^h$ in this way, $\nabla \cdot \mathbf{u}^h = 0$ is automatically satisfied and hence the residual of the continuity equation can be dropped from the least-squares functional. However, a term that penalizes the jump of the stream function must be added to the functional. Furthermore, because velocity is eliminated, the velocity boundary condition must be implemented through the stream function. It is easy to see that $\mathbf{n} \cdot \nabla \times \psi$ involves only tangential derivatives of ψ. Therefore, a Dirichlet boundary condition on the stream-function specifies the normal component of the velocity. We specify the tangential component of the velocity weakly by adding another least-squares term to our functional. As a result, we arrive at the following discontinuous stream function-vorticity-pressure (SVP) least-squares functional:

$$\begin{aligned}
&\widehat{J}^h_{-1}(\psi^h, \omega^h, p^h; \mathbf{f}^h) = \\
&\quad h^2 \left\|\nabla \times \omega^h + \nabla p^h - \mathbf{f}^h\right\|_0^2 + \sum_{K \in \mathcal{K}} \left\|\nabla \times \nabla \times \psi^h - \omega^h\right\|_{0,K}^2 \\
&\qquad + h^{-1} \sum_{e_i \in \mathcal{E}(\Omega)} \left(\alpha_1 \int_{e_i} [(\nabla \times \psi^h) \cdot \mathbf{n}_i]^2 d\ell + \alpha_2 \int_{e_i} [(\nabla \times \psi^h) \times \mathbf{n}_i]^2 d\ell \right) \\
&\qquad + h^{-1} \sum_{e_i \in \mathcal{E}(\Gamma)} |(\nabla \times \psi^h) \times \mathbf{n}_i|^2 d\ell + h^{-3} \sum_{e_i \in \mathcal{E}(\Omega)} \int_{e_i} [\psi^h]^2 d\ell
\end{aligned} \tag{3.8}$$

The weight for the last term of (3.8) is determined by a scaling argument assuming that $\psi \in H^2$ and hence its trace is in $H^{3/2}$. The jump of the stream-function is necessary for elements not adjacent to the boundary since constraining only $[\mathbf{n} \cdot \nabla \times \psi]$ and $[\mathbf{n} \times \nabla \times \psi]$ specifies ψ only up to a constant. Once (3.8) is solved, the velocity is recovered through formula (3.7), i.e., on each element

$$\mathbf{u}^h|_K = \nabla \times \psi^h|_K\,. \tag{3.9}$$

We can view the discontinuous SVP formulation (3.8) as a special case of the discontinuous velocity formulation (3.5) with a specific choice of a *divergence-free* basis. We choose to define this basis through a stream function as in (3.7) primarily because of the simplicity of this choice; however, it should be clear that our approach can easily accommodate any choice of a divergence-free velocity basis.

It is worth pointing out that the discrete least-squares method for the Darcy flow in two-dimensions [7] uses a discontinuous finite element space for the flux defined in a similar manner by

$$\mathbf{V}^h = \nabla(S^h) \oplus \nabla \times (S^h)\,, \tag{3.10}$$

where S^h_D and S^h_N are standard C^0 finite element spaces constrained by zero on the Dirichlet and Neumann portions of the boundary. The key difference is that our approach deals with the discontinuity of the approximating space by including appropriate jump terms and retaining the original differential operators, whereas [7] retains the global inner products but switches to weak discrete differential operators defined using integration by parts.

The use of stream functions is not a novel idea, and has been applied to the Stokes equations [11], however, most research on the SVP formulation is done using finite differences because of the presence of the second derivative. However, in the discontinuous framework, it is not necessary to construct a global $H^2(\Omega)$-conforming finite element space as $\nabla \times \nabla \times \psi$ is only needed locally.

4. Implementation. All of the above methods are implemented using Intrepid [5] and solved using the KLU solver of Amesos [17], both packages of Trilinos [12]. Intrepid is a local framework that implements basis functions for $H^1, H(curl)$, and $H(div)$. Since our formulations are discontinuous, it suffices to choose basis functions to be H^1 on each element and implement the jump terms.

It is easy to convert least squares functionals to an implementable weak form by setting the first directional derivative to zero. For example, the weak form that minimizes (3.5) is to find $(\mathbf{u}^h, \omega^h, p^h) \in X_r^h$, such that

$$\begin{aligned}(\nabla \times \omega^h + \nabla p^h, \nabla \times s^h + \nabla q^h) + \sum_{K \in \mathcal{K}} (\nabla \times \mathbf{u}^h - \omega^h, \nabla \times \mathbf{v}^h - s^h)_{0,K} \\ + \sum_{e_i \in \mathcal{E}(\Omega)} \left(\int_{e_i} [\mathbf{u}^h \cdot \mathbf{n}][\mathbf{v}^h \cdot \mathbf{n}] d\ell + \int_{e_i} [\mathbf{u}^h \times \mathbf{n}][\mathbf{v}^h \times \mathbf{n}] d\ell \right) = (f, \nabla \times s^h + \nabla q^h)_0\end{aligned} \tag{4.1}$$

for all $(\mathbf{v}, s, q) \in [H_0^1(\Omega)]^2 \times H^1(\Omega) \times L_0^2(\Omega)$. The weak form for all other least squares functionals can be obtained in a similar way.

Since $\mathbf{u} = (u_1^h, u_2^h)$ is a vector valued function, each component has separate degrees of freedom and in the cases where $\mathbf{u}^h$ is discontinuous, each element has its own set of degrees of freedom for u_1^h and u_2^h.

4.1. Transformations. All basis functions are defined on the reference element, thus, it is necessary to use the correct transformation. Intrepid provides implementations for the most common transformations; however, non standard transformations such as $\nabla \times \omega$ (curl of a scalar field in two-dimensions) and (for the SVP formulation) $\nabla \times \nabla \times \psi$ are not straightforward. $\nabla \times \omega$ is the curl of a scalar function and hence is an element of $H(div)$. Thus we use `HDIVtransformVALUE` for curls of scalar functions. In two dimensions, using the identity,

$$\nabla \times \nabla \times \psi = -\psi_{xx} - \psi_{yy} \tag{4.2}$$

it follows that on a reference element, we can compute $\nabla \times \nabla \times \psi$ by using `OPERATOR_D2` which computes all second derivatives of ψ. Once $\nabla \times \nabla \times \psi$ is computed for the reference element, it is necessary to transform to the physical element. This is done by noting that $\nabla \times \psi \in H(div)$, and $\nabla \times \mathbf{v}$, for a vector valued function $\mathbf{v}$, is a *rotated divergence* and hence `HDIVtransformDIV` transformation is used.

4.2. Boundary conditions. In all of our tests, we use the velocity boundary condition where $\mathbf{u}|_{\partial\Omega} = \mathbf{u}_D$ is specified on the entire boundary. We set the pressure to 0 at a single point on the boundary. Since the basis in Intrepid is interpolatory, the boundary conditions are set strongly by specifying

$$\begin{array}{ll} \mathbf{u}(x_i)\mathbf{u}_D(x_i) & \forall x_i \in \partial\Omega \\ p(x_0)0 & \end{array} \tag{4.3}$$

This is done by defining a vector u_0 that is zero for all degrees of freedom corresponding to interior points and equal to $\mathbf{u}_D$ at the boundary degrees of freedom. We then set

$$\mathbf{b} \leftarrow \mathbf{b} - A\mathbf{u_0} \tag{4.4}$$

Each row and column of A corresponding to a boundary degree of freedom is set to zero and the diagonal is set to 1.

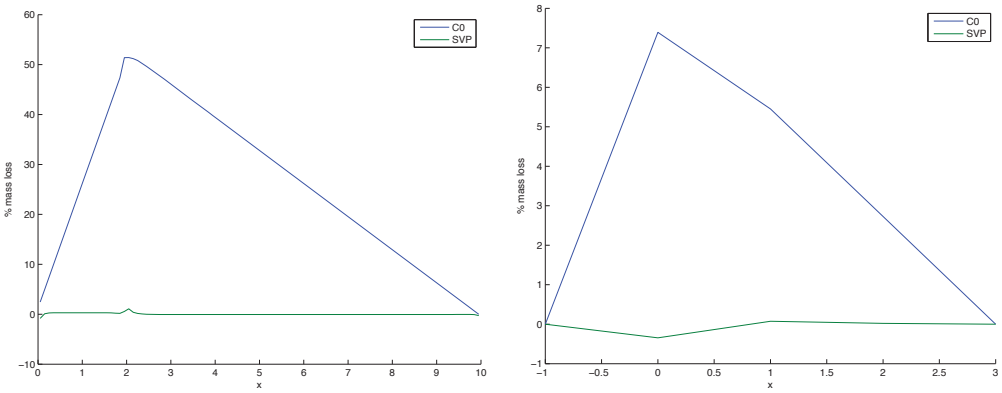

FIG. 5.1. *Comparison of mass loss of for the backward-facing step (left panel) and the flow past a cylinder (right panel) test problems. Blue line represents weighted L^2 formulation (2.19), green line is SVP formulation (3.8).*

5. Numerical examples. Because the discontinuous SVP formulation (3.8) does not include the velocity some care must be exercised in setting the velocity boundary condition for our two test problems. In the case of the backward step, recall that the boundary condition is given by (2.14). Because on Γ_{in} and Γ_{out} velocity is only a function of y, the $\mathbf{u}_1$ component is integrated to obtain an equivalent boundary condition on the stream function:

$$\psi_{in} = -\frac{8}{3}y^3 + 6y^2 - 4y + C_1, \quad \psi_{out} = \frac{y^2}{2} - \frac{y^3}{3} + C_2 \tag{5.1}$$

The constants C_1 and C_2 are chosen so that $\mathbf{u}_{in}(0.5) = \mathbf{u}_{out}(0)$ and $\mathbf{u}_{in}(1) = \mathbf{u}_{out}(1)$. The top and bottom walls are then chosen to be constants equal to $\mathbf{u}_{in}(1)$ and $\mathbf{u}_{in}(0.5)$ respectively. Likewise, the equivalent stream function boundary conditions for the second domain, Figure 2.2, with velocity boundary conditions (2.15) are

$$\psi_{in} = \psi_{out} = \psi_{wall} = y - \frac{y^3}{3}. \tag{5.2}$$

However, setting the boundary conditions in this way enforces only the normal component of the velocity. In our test cases, the tangential velocity vanishes on all boundaries. We set the tangential velocity weakly by including

$$\|\mathbf{n} \times \nabla \times \psi\|^2_{1/2,\Gamma} \approx h^{-1} \|\mathbf{n} \times \nabla \times \psi\|^2_{0,\Gamma} = h^{-1} \sum_{e_i \in \mathcal{E}(\Gamma)} \int_{e_i} |\mathbf{n} \times \nabla \times \psi|^2 d\ell \tag{5.3}$$

in the least squares functional (3.8).

The resulting mass loss for (3.8) is summarized in Figure 5.1 and it is seen that mass conservation is significantly improved. Indeed, for the backward facing step, the maximum mass loss is less than 1.09% with most of the mass loss centralized at the reentrant corner. On the rest of the domain, the solution is basically conserved over any closed subdomain. This is a dramatic improvement compared to (2.19). For the channel flow with cylinder cutout, the mass conservation is also improved with a slight mass *gain* of 0.34% at the opening of the cylinder. Compared with (3.5), the stream function formulation is able to achieve better mass conservation than (2.19)–recall that no matter how α_1 and α_2 were chosen, the mass conservation could not improve past the weighted L^2 formulation.

The velocity fields of each formulation are visualized in Figures 5.2 and 5.5 and in the case of the backward facing step, the mass loss for (3.5) is clearly visible. For the SVP

formulation, the propagation of the parabolic profile of the inflow is clearly seen throughout the domain. In the case of the weighted L^2 formulation, the parabolic profile diminishes–symbolic of the 50% mass loss. From the additional figures (5.3-5.8), it can also be seen that the pressure and vorticity are more accurately captured with the stream function formulation.

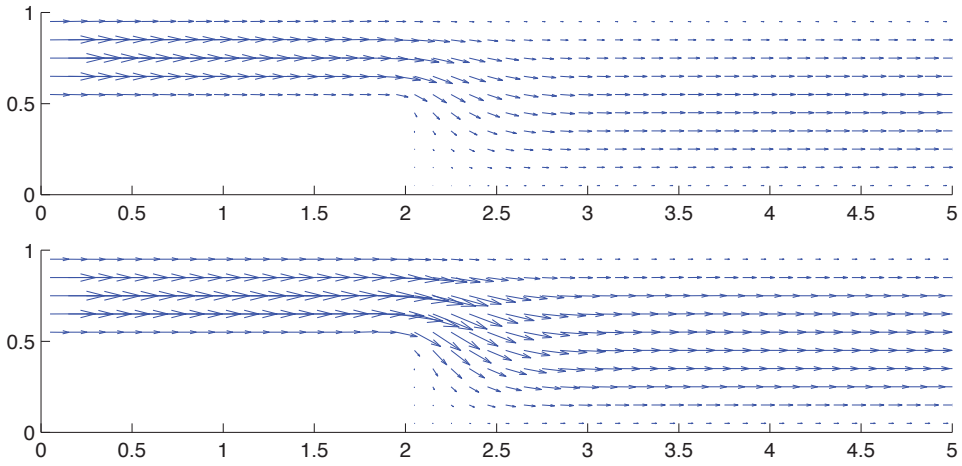

FIG. 5.2. *Velocity plot of C^0 (2.19) (top) and SVP (3.8) (bottom) for the backward-facing step.*

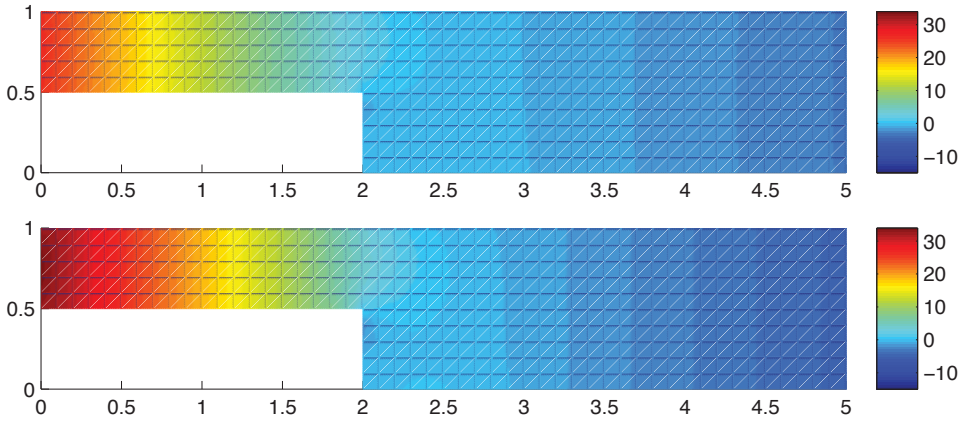

FIG. 5.3. *Pressure plot of C^0 (2.19) (top) and SVP (3.8) (bottom) for the backward-facing step.*

We considered using divergence free bases on each element, because of the necessity to choose the *correct* weights α_1 and α_2 in (3.5). However, it was not possible to choose a single set of weights that is optimal for all test cases. In the case of (3.8), only one set of weights is used and proved to be effective.

6. Conclusion. In this report we have formulated new discontinuous velocity LSFEMs for the Stokes equations as a means to improve mass conservation. These new methods were compared with a provably optimal norm equivalent weighted L^2 least squares formulation. The immediate discontinuous velocity formulation was found to not be robust as depending on the problem, different weights were required. As a result, a local divergence free basis for the velocity was introduced with the use of a stream function. The stream function approach

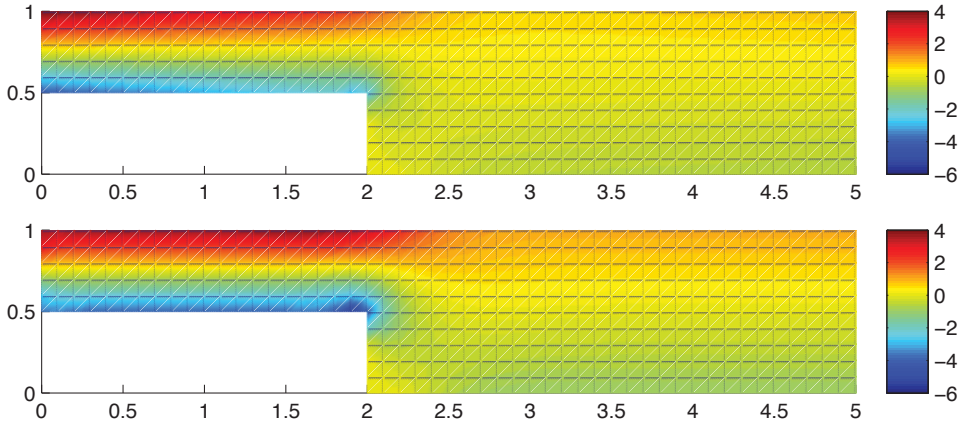

FIG. 5.4. *Vorticity plot of C^0 (2.19) (top) and SVP (3.8) (bottom) for the backward-facing step.*

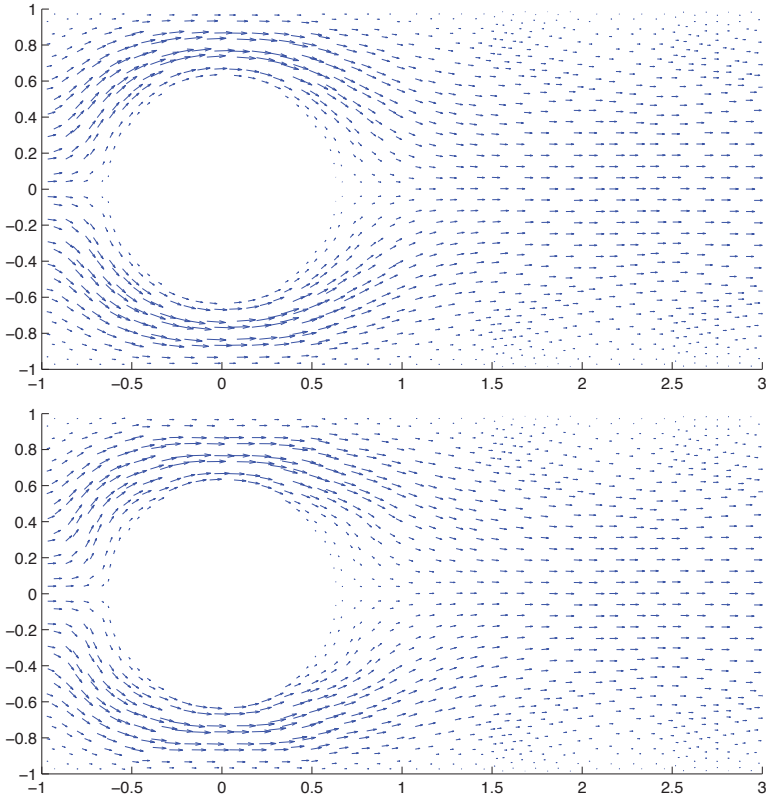

FIG. 5.5. *Velocity plot of C^0 (2.19) (top) and SVP (3.8) (bottom) for the cylinder channel.*

proved to be robust as only one set of weights, derived from Sobolev theory, allowed the resulting solution to be almost entirely mass conservative.

The proposed approach is very flexible and can be easily applied to other LSFEMs based on the VVP or other first-order Stokes systems. For example, it is trivial to extend (3.8) to a discrete negative-norm method, or to a method which uses velocity gradient, velocity and pressure as dependent variables.

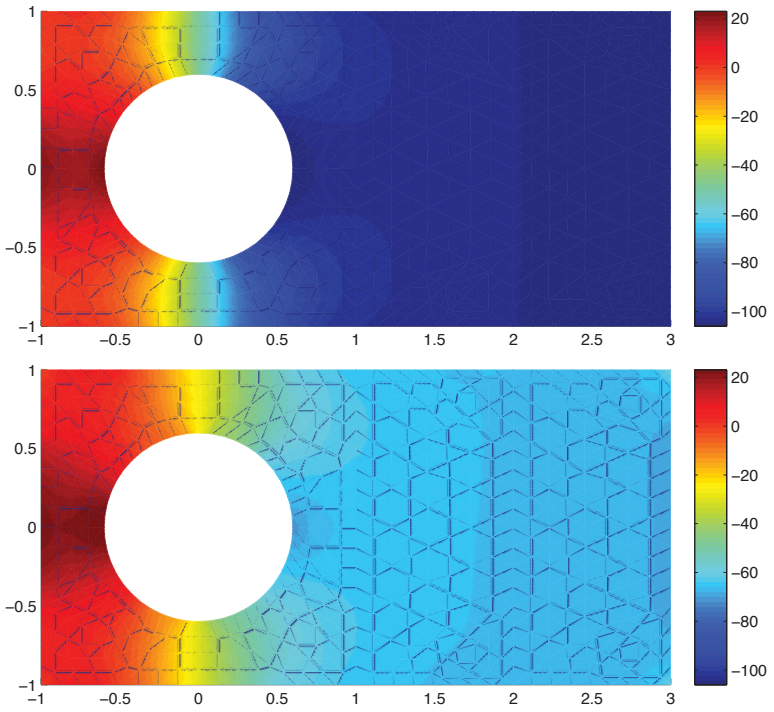

FIG. 5.6. *Pressure plot of C^0 (2.19) (top) and SVP (3.8) (bottom) for the cylinder channel.*

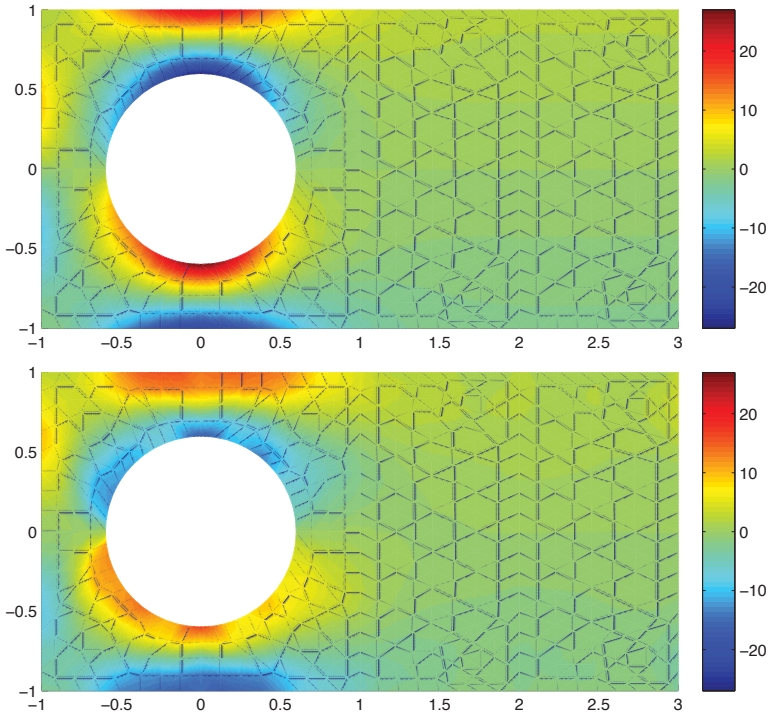

FIG. 5.7. *Vorticity plot of C^0 (2.19) (top) and SVP (3.8) (bottom) for the cylinder channel.*

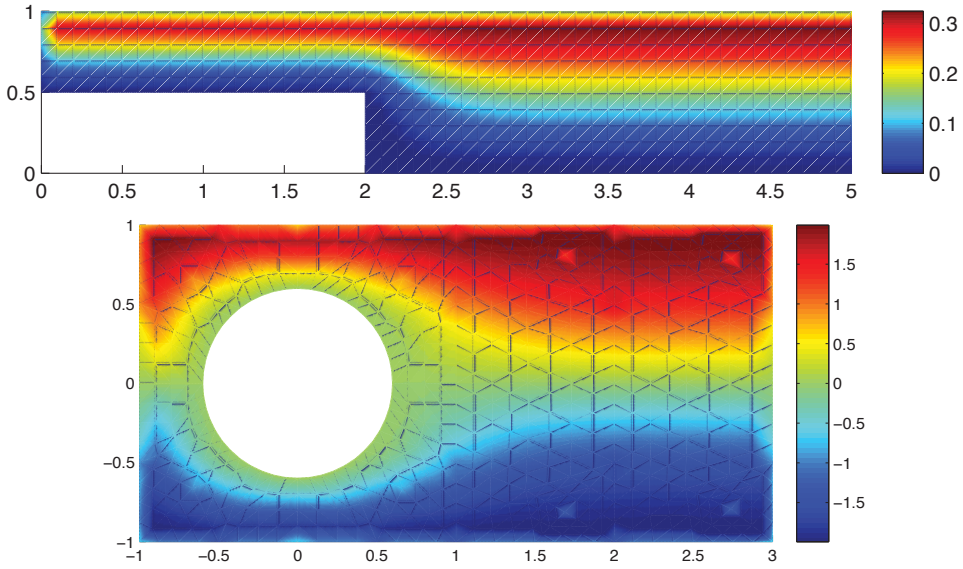

FIG. 5.8. *Stream function for backward step (top) and cylinder channel (bottom).*

Future work in the area includes theoretical studies of the well-posedness of discontinuous formulations and an implementation of (3.8) using cubic elements for the stream function. This allows the velocity, the curl of the stream function, to be quadratic–satisfying the minimal degree requirement of the parent C^0 least-squares formulation.

REFERENCES

[1] P. BOCHEV AND D. DAY, *Analysis and computation of a least-squares method for consistent mesh tying.*, J. Comp. Appl. Math, 218 (2008), pp. 21–33.

[2] P. BOCHEV AND M. GUNZBURGER, *Analysis of least-squares finite element methods for the Stokes equations*, Math. Comp., 63 (1994), pp. 479–506.

[3] ———, *Least-squares finite element methods*, Springer, 2009.

[4] ———, *A locally conservative mimetic least-squares finite element method for the Stokes equations*, in Proceedings of LSSC 2009, I. Lirkov, S. Margenov, and J. Wasniewski, eds., vol. 5910 of Springer Lecture Notes in Computer Science, 2009, pp. 637–644.

[5] P. BOCHEV, D. RIDZAL, AND K. PETERSON, *Intrepid: Interoperable Tools For Compatible Discretizations*. http://trilinos.sandia.gov/packages/intrepid/, 2010.

[6] P. BOLTON AND R. THATCHER, *On mass conservation in least-squares methods*, J. Comput. Phys., 203 (2005), pp. 287–304.

[7] Z. CAI AND B. SHIN, *The discrete first-order system least squares: the second-order elliptic boundary value problem*, SIAM J. Numer. Anal., (2002), pp. 307–318.

[8] Y. CAO AND M. GUNZBURGER, *Least-squares finite element approximations to solutions of interface problems*, SIAM J. Numer. Anal., 35 (1998), pp. 393–405.

[9] C. CHANG AND J. NELSON, *Least-squares finite element method for the Stokes problem with zero residual of mass conservation*, SIAM J. Numer. Anal., 34 (1997), pp. 480–489.

[10] J. DEANG AND M. GUNZBURGER, *Issues related to least-squares finite element methods for the Stokes problem*, SIAM J. Numer. Anal., 35 (1998), pp. 878–906.

[11] U. GHIA, K. GHIA, AND C. SHIN, *High-re solutions to incompressible flow using the Navier-Stokes equations and a multigrid method*, J. Comput. Phys., 48 (1982), pp. 387–411.

[12] M. HEROUX, R. BARTLETT, V. HOWLE, R. HOEKSTRA, J. HU, T. KOLDA, R. LEHOUCQ, K. LONG, R. PAWLOWSKI, E. PHIPPS, A. SALINGER, H. THORNQUIST, R. TUMINARO, J. WILLENBRING, AND A. WILLIAMS, *An Overview of Trilinos*, Tech. Rep. SAND2003-2927, Sandia National Laboratories, 2003.

[13] J. HEYS, E. LEE, T. MANTEUFFEL, AND S. MCCORMICK, *On mass-conserving least-squares methods*, SIAM J. Sci. Comput, 28 (2006), pp. 1675–1693.

[14] ———, *An alternative least-squares formulation of the Navier-Stokes equations with improved mass conservation*, J. Comput. Phys, 226 (2008), pp. 994–1006.

[15] J. Heys, E. Lee, T. Manteuffel, S. McCormick, and J. Ruge, *Enhanced mass conservation in least-squares methods for Navier-Stokes equations*, SIAM J. Sci. Comput., 31 (2009), pp. 2303–2321.

[16] J. Pontaza and J. Reddy, *Space-time coupled spectral/hp least-squares finite element formulations for the incompressible Navier-Stokes equations*, J. Comput. Phys., 197 (2004), pp. 418–459.

[17] M. Sala, K. Stanley, and M. Heroux, *Amesos: A set of general interfaces to sparse direct solver libraries*, in Proceedings of PARA'06 Conference, Umea, Sweden, 2006.